Biochimica et Biophysica Acta 1842 (2014) 1742–1754

Contents lists available at ScienceDirect

Biochimica et Biophysica Acta

journal homepage: www.elsevier.com/locate/bbadis

Opposite angiogenic outcome of curcumin against ischemia and Lewis lung cancer models: in silico, in vitro and in vivo studies

Shengjun Fan [1], Yan Xu [1], Xin Li, Lu Tie, Yan Pan, Xuejun Li *

State Key Laboratory of Natural and Biomimetic Drugs, Department of Pharmacology, School of Basic Medical Sciences, Peking University Health Science Center, Beijing Key Laboratory of Tumor Systems Biology, Peking University, Beijing 100191, China

ARTICLE INFO

Article history:
Received 11 January 2014
Received in revised form 30 April 2014
Accepted 17 June 2014
Available online 23 June 2014

Keywords:
Curcumin
Angiogenesis
Ischemia and lung cancer model
Neutrophil elastase

ABSTRACT

The aim of this study was to investigate the angiogenic effects of curcumin on an ischemia and lung cancer model. To induce ischemia combined with lung cancer models, unilateral femoral arteries of C57BL/6 mice were disconnected on one side of the mouse and Lewis lung carcinoma (LLC) cells were xenografted on the opposite side. Angiogenic effects and underlying mechanisms associated with curcumin were investigated. Molecular target(s), signaling cascades and binding affinities were detected by Western blot, two-dimensional gel electrophoresis (2-DE), computer simulations and surface plasmon resonance (SPR) techniques. Curcumin promoted post-ischemic blood recirculation and suppressed lung cancer progression in inbred C57BL/6 mice via regulation of the HIF1α/mTOR/VEGF/VEGFR cascade oppositely. Inflammatory stimulation induced by neutrophil elastase (NE) promoted angiogenesis in lung cancer tissues, but these changes were reversed by curcumin through directly reducing NE secretion and stimulating α1-antitrypsin (α1-AT) and insulin receptor substrate-1 (IRS-1) production. Meanwhile, curcumin dose-dependently influenced endothelial cells (EC) tube formation and chicken embryo chorioallantoic membrane (CAM) neovascularization. Curcumin had opposite effects on blood vessel regeneration under physiological and pathological angiogenesis, which was effected through negative or positive regulation of the HIF1α/mTOR/VEGF/VEGFR cascade. Curcumin had the promise as a new treatment modality for both ischemic conditions and lung cancer simultaneously in the clinic.

1. Introduction

Angiogenesis inhibition elicits detrimental effects on tumor proliferation [1], whereas revascularization is recognized as a better choice for ischemic disorders [2–5]. Unfortunately, unselective stimulation of vascular endothelial cells (EC) results in angiogenic problems that can lead to carcinogenesis, inflammation or hypertension [6]. With the increase of the aging population, concerns have arisen recently for individuals with multiple diseases. One important current area of concern is the need for new knowledge regarding the clinical management of ischemic insult and lung cancer occurring in the same patient at the same time. Thus, novel agents that promote angiogenesis in response to ischemic ailments and block malignant tumor growth are urgently needed [7].

Owing to reduce side effects compared with some conventional chemotherapy, plant-derived ingredients have been extensively used against malignancies [8]. They are recommended as a feasible therapy for advanced cancer in combination with radiation therapy. Curcumin, a dietary pigment in curry, has been characterized as benign and well tolerated even at extremely high doses [9]. It has also been proposed as a multitarget drug candidate and used as a template for drug design [10,11]. Conclusive evidence regarding the beneficial significance of curcumin as a vascular-promoting compound against ischemic insult has been reviewed [12,13]. As well, curcumin has been shown to exert

Abbreviations: 2-DE, two-dimensional gel electrophoresis; α1-AT, α1-antitrypsin; Akt, serine/threonine-protein kinase; BCIP, 3-bromo-4-chloro-5-indolyl phosphate; BSA, bovine serum albumin; CAM, chicken embryo chorioallantoic membrane; EC, endothelial cells; ECCM, epithelial cell conditioned medium; ECGS, endothelial cell growth supplement; ELISA, enzyme-linked immunosorbent assay; ESI-Q-TOP-MS, electrospray ionization quadrupole/time of flight mass spectrometry; FBS, fetal bovine serum; GAD, genetic association database; GRNs, gene regulatory networks; hNE, human neutrophil elastase; HIF1α, hypoxia-inducible factor 1-alpha; HUVEC, human umbilical vein endothelial cells; i.g., intragastric administration; IRS-1, insulin receptor substrate-1; LLC, Lewis lung cancer; MTS, 3-(4,5-dimethylthiazol-2-yl)-5-(3-carboxymethoxyphenyl)-2-(4-sulfophenyl)-2H-tetrazolium; MVD, microvessel density; mTOR, mammalian target of rapamycin; MRM, multiple reaction monitoring; NBT, nitro blue tetrazolium; NE, neutrophil elastase; OMIM, Online Mendelian Inheritance in Man; PCR, polymerase chain reaction; PDB, Protein Data Bank; s.c., subcutaneous; RU, response units; SEM, standard error of measurement; SPR, surface plasmon resonance; VEGF, vascular endothelial growth factor; VEGFR, vascular endothelial growth factor receptor

* Corresponding author at: Department of Pharmacology, School of Basic Medical Sciences, Peking University Health Science Center, No. 38 Xueyuan Road, Haidian District, Beijing 100191, China. Tel./fax: +86 10 82802863.

E-mail addresses: herryvan@sohu.com (S. Fan), yan_xu81@yahoo.com.cn (Y. Xu), lixin0837@163.com (X. Li), tielu@bjmu.edu.cn (L. Tie), pannay26@bjmu.edu.cn (Y. Pan), xjli@bjmu.edu.cn (X. Li).

[1] These authors contributed equally to this work.

http://dx.doi.org/10.1016/j.bbadis.2014.06.019
0925-4439/

anti-tumorigenic effects towards a number of different cancers e.g. adenoid crystic carcinoma, lung cancer and breast cancer [14–18]. Although the multifunctional nature of curcumin towards ischemic conditions or cancer has been well documented individually, the opposite angiogenic effects of curcumin have not been studied simultaneously in the same model. Recently, neutrophil elastase (NE) was reported to be a pro-inflammatory cytokine associated with cancer initiation and progression [19]. Endogenous NE could potentially accelerate blood vessel regeneration in malignant disease [20]. Physiological production of NE was principally stimulated by neutrophils or alveolar macrophages, and eliminated by α1-antitrypsin (α1-AT) [21]. The decreased α1-AT might come from cancer tissues, from which endogenous NE was secreted [22,23].

The purpose of our present study is to gain a further insight into the dual angiogenic effect of curcumin in a combined ischemic insult and Lewis lung cancer (LLC) model, and to investigate if the presence of NE in the LLC tissue resulted in the opposite regulation of HIF1α/mTOR/VEGF/VEGFR cascade in this model. A better understanding of the multiple functions of curcumin may shed new light on the simultaneous clinical management of ischemic illnesses and lung cancer.

2. Materials and methods

2.1. Cell culture and ethics statement

The *in vitro* experiments on human umbilical vein endothelial cells (HUVEC) complied with the principles outlined in the Declaration of Helsinki [24]. After obtaining written informed consent, HUVEC was isolated from human umbilical cord from healthy volunteers according to a protocol approved by the Ethics Review Board of the Hospital of Beijing Obstetrics and Gynecology Hospital in China. Cells were taken from the primary culture and incubated in epithelial cell conditioned medium (ECCM, GIBCO-BRL, Grand Island, NY, USA) basal media supplemented with growth supplements including 20% fetal bovine serum (FBS, Hyclone, Logan, UT, USA), 40 units/mL heparin (Inalco Spa, Milano, Italy), 50 μg/mL Endothelial Cell Growth Supplement (ECGS, GIBCO-BRL, Grand Island, NY, USA), 2 mM L-glutamine, 0.4 units/mL insulin, 100 units/mL penicillin and 100 μg/mL streptomycin (Biodee Biotechnology Co., Beijing, China) in a humidified incubator (Sanyo Electric Co., Ltd., Tokyo, Japan) with 5% CO_2 at 37 °C.

For *in vivo* study, the LLC cell line was purchased from Cell Resource Center of Peking Union Medical College (Beijing, China) and maintained in Dulbecco's modified Eagle's medium (DMEM, GIBCO-BRL, Grand Island, NY, USA) with 10% FBS, 100 units/mL penicillin and 100 μg/mL streptomycin. Cells were maintained at 37 °C with 5% CO_2 and proper humidity.

2.2. Ischemia and LLC mice model

Experimental animal facilities and animal experiments were carried out in strict accordance with the European Community guidelines for the use of experimental animals and approved by the Peking University Committee on Animal Care and Use (Permit Number: IRB00001052-5135). All surgeries were performed under deep anesthesia with 20% sodium pentobarbital (Sagatal, Rhone Merieux Ltd., Harlow, Essex, UK), and all efforts were made to minimize animal suffering.

Wild-type C57BL/6 female mice weighing 18–20 g were provided by Peking University Health Science Center Institutional Animal Care (Grade II, Certificate No. 11-00-0004). Ischemia combined with LLC tumor models were established as previously described [25]. LLC tumor tissue (tumor (g): physiological saline (mL) = 1:3, w/v) was homogenized and 0.2 mL of the suspension (approximately 6×10^6 cells) was injected subcutaneously (s.c.) into the right flank fold region of the mouse with the left femoral arteries disconnected on the same day. Mice (n = 8–10 per group) were randomly divided into three groups and saline (vehicle), 100 or 300 mg/kg curcumin (purity ≥ 98.0%, Sigma-Aldrich, St. Louis, MO, USA) was administrated every day. On day 22, mice were killed by decapitation 30 min under deep anesthesia. Ischemic muscles and lung cancer tissues were rinsed with chilled PBS twice, embedded in an optimal cutting temperature compound (Tissue-Tek, Miles Scientific, Naperville, IL, USA) for immunostaining assay or frozen in liquid nitrogen for Western blot, real-time PCR, ELISA and LC-MS/MS analysis. All samples were stored at −80 °C before use.

2.3. Laser Doppler analysis

Mice were placed ventral side up under general anesthesia. Limbs were immobilized and scanned using a laser-Doppler blood-flow Imager (PeriScan PIM3, Perimed, Stockholm, Sweden). Measurements were done immediately after femoral artery and tumor implantation surgery at 7, 14 and 21 days on mice with or without curcumin treatment. The relative morphology of the perfusion data was photographed and the blood flow recovery index was calculated according to the formula: blood flow recovery index = [blood flow in the ischemic hind limb (left)/blood flow in the normal limb (right)] * 100%. To determine the reproducibility of measurements, scans were performed in triplicate and the results of six or eight independent mice were used for statistical analysis.

2.4. Immunohistochemistry

An immunohistochemistry assay for microvessel density (MVD) was performed using CD31 (1:1000, Cell Signaling, Beverly, MA, USA) as previously described [26]. Tissues were harvested, and embedded in an optimal cutting temperature compound. Frozen tissue sections of 6 μm thick were incubated at 4 °C for 12 h with CD31 primary antibody. Sections were rinsed 3 times with phosphate-buffered saline (PBS) and incubated for 10 min in bovine serum albumin (BSA, Hyclone, Logan, UT, USA) to block the nonspecific proteins. After incubating with the secondary antibody used for CD31 (peroxidase-conjugated goat anti-mouse IgG) for 1 h at room temperature, slides were counterstained with diaminobenzidine and photographed. MVD (%) was calculated from the ratio of CD31 positive staining area (positive brown stain) to the total observation area in the viable region. Six fields per section (0.5 mm^2) were randomly analyzed and the positive staining areas were calculated using Image-Pro Plus (Media Cybernetics, Silver Spring, MD, USA).

2.5. Capillary-like tube formation assay

96-well plates (Corning Costar Corp., Cambridge, MA) were coated with 50 μL of matrigel (BD Biosciences, Franklin Lakes, NJ) and incubated at 37 °C for 30 min [27]. HUVEC was transplanted to the 96-well plates with a destiny of 1×10^5 cells/well. Curcumin dissolved in low serum medium (1% FBS) was added to each well at a final concentration of 0.1, 0.3, 1, 3 and 10 μM. After 4 h of incubation, tube morphology was recorded. Each experiment was repeated in triplicate and the tube length was assessed by Image-Pro Plus 6.0 software (Media Cybernetics, Silver Spring, Maryland, USA).

2.6. Chicken chorioallantoic membrane (CAM) assay

Specific-pathogen-free (SPF) Leghorn fertile chicken eggs (Beijing Merial Vital Laboratory Animal Technology Co. Ltd., Beijing, China) were obtained from 40 weeks old Single Comb White Leghorn chickens and maintained in a humidified environment at 37.5 °C until 6 days of incubation [28]. A hole with a diameter of 10 × 10 mm was subsequently broken and continued to incubate for another 1 day. On day 7, curcumin (0, 0.3, 1, 3, 10 and 30 μM) dissolved in DMEM was then added to a microbial testing disk and placed onto CAM. After 72 h of incubation, the digitized CAM images were recorded.

2.7. Disease-gene network construction

Genes associated with ischemia and lung cancer were screened from Online Mendelian Inheritance in Man (OMIM, http://www.ncbi.nlm.nih.gov/omim), Genetic Association Database (GAD, http://www.geneticassociationdb.nih.gov/) and GeneCards (http://www.genecards.org). To infer a network-based pathway analysis of ischemia and lung cancer, Agilent LitSearch tool in Cytoscape environment (http://www.cytoscape.org) was utilized for gene excavation [29]. For Network Analyzer application, self-loops and duplicated edges were ignored.

2.8. Pathways enrichment analysis

After intersecting with Network Merge plugin, predominant gene regulatory networks (GRNs) associated with ischemia and lung cancer were clustered by molecular complex detection (MCODE) algorithm [30]. For pathways enrichment analysis, ToppGene was employed as the gene set categories [31].

2.9. Two-dimensional gel electrophoresis analysis

Serum from mice with or without curcumin treatment was quantified for protein by the bicinchoninic acid (BCA) assay. Two-dimensional gel electrophoresis (2-DE) analysis was carried out on a Bio-Rad 2-DE system (Bio-Rad Laboratories, Hercules, CA, USA) following the Bio-Rad handbook. Protein samples of 75 μg were separated for isoelectric focusing (IEF) in the first dimension using precast immobilized pH gradient strips (IPG strips, Amersham Pharmacia Biotechnology Inc., New Jersey, USA, pH range: 3 to 10 linear, 18 cm). Afterwards, the IPG strips were equilibrated for 15 min with the equilibration solution consisting of 50 mM Tris–HCl, pH6.8, 6 M urea, 30% glycerol and 2% SDS (Sigma-Aldrich, St. Louis, MO, USA). 20 mM DTT included in the first equilibration solution, and 2% (w/v) iodoacetamide (Merck, Darmstadt, Germany) was added in the second equilibration step to alkylate thiols. Subsequently, SDS-PAGE gels for electrophoresis were applied for the second dimension based upon Ettan Dalt II system (Amersham Pharmacia Biotechnology Inc., USA) with the running SDS/Tris buffer consisting with 0.5% agarose at a constant power (2.5 W/gel for 40 min and 15 W/gel for 6 h) at room temperature. Gels were stained with silver nitrate based on the Silver-Staining Plus kit reagent (Amersham Pharmacia Biotechnology Inc., USA) according to the manufacturer's protocols.

2.10. Image analysis and protein identification by ESI-Q-TOP-MS

Stained 2-DE gels were scanned and analyzed using PDQuest software (Bio-Rad, Hercules, CA, USA). Significantly over-represented protein spots ($p < 0.05$ and fold change ≥ 2.0) were excised manually from gels and dissolved in a digestive solution (0.5% TFA). Proteins of interest were analyzed by an eletrospray ionization quadrupole/time of flight mass spectrometry (ESI-Q-TOP-MS, Waters, Micromass, Manchester, USA). For protein identification, analysis was performed using the Mascot software (http://www.matrixscience.com/). Each experiment was performed in triplicate and results from three independent experiments were utilized for statistical analysis.

2.11. Molecular docking and dynamics simulation

The molecular docking procedure between NE and curcumin was appraised using CDOCKER in Discovery Studio™ 2.5 (DS, Accelrys, San Diego, CA, USA) environment [32]. For ligand preparation, 2-D structure of curcumin was produced by KegDraw software. Forcefield was applied and binding energy was minimized before the docking procedure. As for receptor preparation, X-ray crystal structure of NE was downloaded from the Protein Data Bank (PDB, http://www.rcsb.org/) with the code number 1B0F. Further, a ligand-based similarity search scheme was employed and the docking protocol was performed as a default setting to avoid a potential reduction in docking accuracy.

Molecular dynamics simulations of NE and curcumin were performed using the standard dynamics cascade protocol in DS. The initial structures of those two simulations were the results of the ligand-receptor complex with the lowest binding energy. The complex was solvated with water in a cubic box with an explicit periodic boundary model to stimulate the environment inside the cell. After creating harmonic restraint, a standard dynamics cascade was performed including minimization, heating, equilibration and production dynamics.

2.12. Surface plasmon resonance analysis

The *in vitro* binding affinity assay between NE and curcumin was appraised by a Biacore 3000 surface plasmon resonance (SPR, Biacore AB, Uppsala, Sweden). Recombinant human NE (hNE) protein with purity greater than 98.0% (Catalog number 423681) was purchased from Merck KGaA (Darmstadt, Germany). Pipelines and chip were pretreated with PBS-EP running buffer (0.01 M HEPES, 0.15 M NaCl, 3 mM EDTA, 0.005% Surfactant P20 and deionized water, pH 7.4). For SPR analysis, NE was immobilized on a CM_5 sensor chip with pH 5.5. Analysis was performed at a flow rate of 10 μL/min at 25 °C. Incremental curcumin doses (7.5, 15, 30, 60 and 120 μM) dissolved in running buffer were injected into the channels, and binding responses were recorded for 300 s in succession. Binding responses were recorded continuously with response units (RU) values. The association (k_a) and dissociation (k_d) rate constants were elevated by BIA evaluation software (Biacore AB, Uppsala, Sweden).

2.13. Western blot analysis

Tissues samples were washed twice with chilled PBS and homogenized. After centrifuging and boiling at 100 °C for 5 min, proteins from total cell lysates were separated by SDS-PAGE and transferred to a PVDF membrane (Bio-Rad). For Western blot analysis of Akt/p-Akt (1:1000, Cell Signaling, Beverly, MA, UK), mTOR/p-mTOR (1:1000, Cell Signaling, Beverly, MA, UK), HIF1α (1:1000, Bioss Biotechnology, Beijing, China), VEGFR (1:1000, Bioss Biotechnology, Beijing, China), α1-AT (1:1000, Santa Cruz, CA, USA), NE (1:1000, Santa Cruz, CA, USA), IRS-1 (1:500, Santa Cruz, CA, USA), GAPDH (1:10,000, Sigma-Aldrich, St. Louis, MO, USA) and β-actin (1:10,000, Sigma-Aldrich, St. Louis, MO, USA), the primary antibodies used in the experiment were probed and incubated overnight at 4 °C, followed by secondary antibody reactions with AP-labeled IgG. The detection was evaluated by the 3-bromo-4-chloro-5-indolyl phosphate (BCIP) and nitro blue tetrazolium (NBT) reaction (Amresco, Solon, OH, USA).

2.14. RNA isolation and quantitative real-time PCR

LLC tissues were homogenized, and total RNA was extracted using TRIzol reagent (Invitrogen, Carlsbad, CA, USA). The primers used for amplifying fragments are as follows: VEGFR (sense primer, 5′-GCCTACCT CACCTGTTTCCTG-3′); (anti sense primer, 5′-TTGTTCCTGTCTTCCAGAG-3′), β-actin (sense primer, 5′-TGCGTGACATCAAAGAGAAG-3′); (anti sense primer, 5′-GATGCCACAGGATTCCATA-3′). For the quantification of VEGFR and β-actin, the cycling protocol consisted of an initial 5 min denaturation at 95 °C, followed by 45 cycles of denaturation at 95 °C for 10 s and extension at 60 °C for 1 min. Reactions were performed using LightCycler (Roche Diagnostics, Mannheim, Germany) with SYBR™ Green (Perkin-Elmer, Foster City, CA, USA).

2.15. Enzyme-linked immunosorbent assay

After 21 days of treatment with curcumin (100 and 300 mg/kg/day), enzyme-linked immunosorbent assay (ELISA) was performed using a VEGF ELISA kit (Boster Biotechnology, Wuhan, Hubei, China) per the

manufacturer's instructions. Microtiter plates were coated overnight with anti-VEGF mAb and blocked by 5% BSA. 100 μL of the homogenate including biosamples or standard were added after washing with PBS. Plates were incubated for 2 h at room temperature and 100 μL of anti-VEGF polyclonal antibody was added. The reaction was determined on a Vmax plate reader at 492 nm.

2.16. Statistical analysis

Significances of difference between two groups were evaluated by a Student's unpaired *t* test and analysis of variance (ANOVA) for comparisons among multiple groups using SPSS version 18.0 (SPSS Inc., Chicago, IL, USA). All data are expressed as mean ± standard error of measurement (SEM).

3. Results

3.1. Curcumin supplements blood-flow in the ischemic hind limb, but suppresses lung cancer progression

To explore the blood-flow restorative capacity of curcumin against ischemic insult, we first quantified the blood-flow restoration in the ischemic hind limb over a 21 day period. Results showed a great viability of blood-flow recovery capacity, which could be shown to occur in a dose-response manner as shown in Fig. 1A. During the first 7 days, blood-flow recovered slightly over that of the vehicle. As time went by, curcumin at both low and high doses significantly enhanced blood-flow in the ischemic hind limb to day 22 (Fig. 1B). The evidence from laser Doppler blood-flow imaging indicates curcumin can

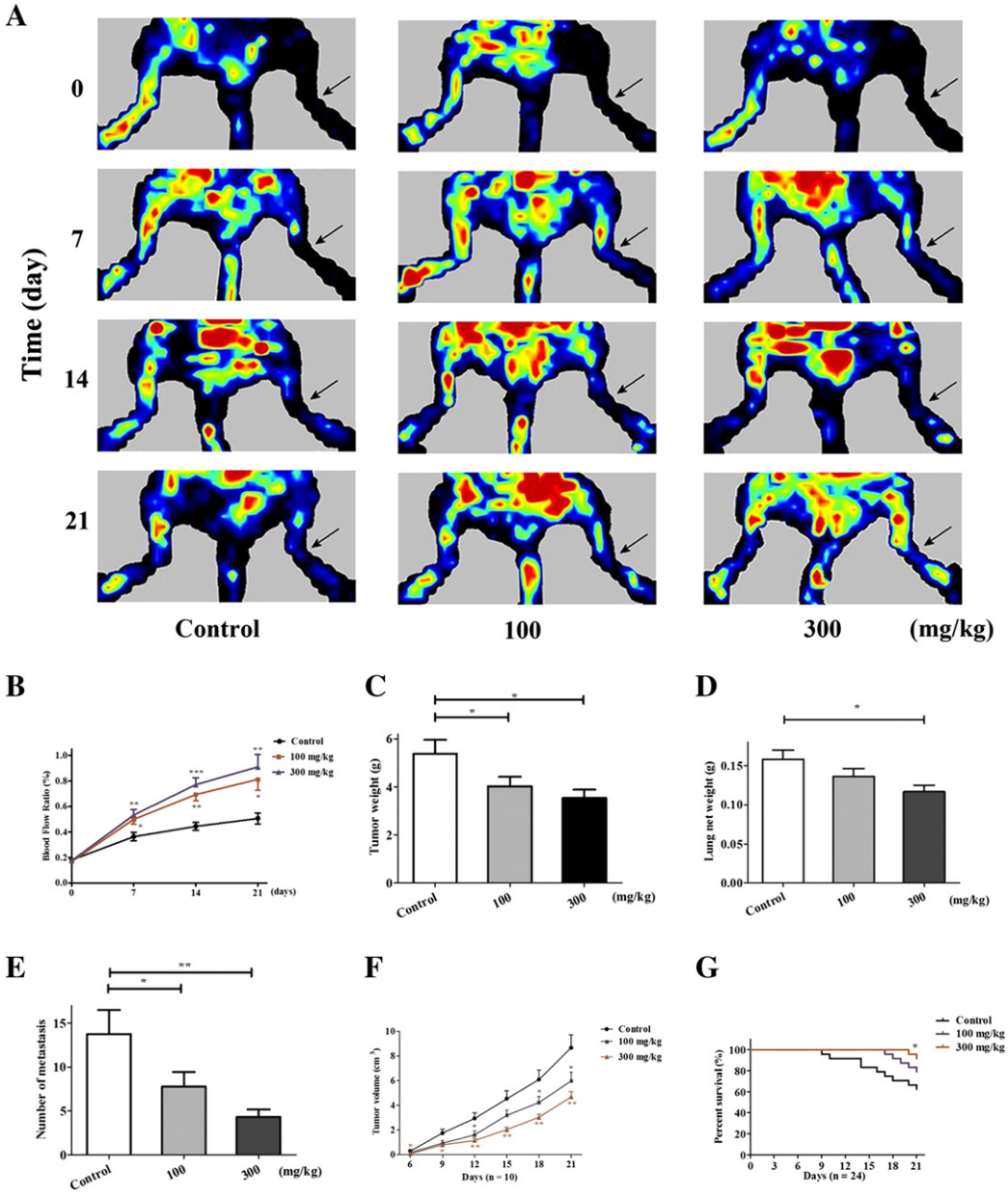

Fig. 1. Blood-flow restoration and anti-cancer activity of curcumin in an ischemic hind limb model combined with a Lewis lung cancer model in the same mouse. (A) Images of the blood-flow restoration in the ischemic hind limb (arrow). (B) Statistical results of blood-flow restoration assay. (C) Effect of curcumin on tumor weight. (D) Effect of curcumin on the wet weight of mouse lung. (E) Statistical results for number of metastasis of Lewis Lung cancer. (F) Effect of curcumin on Lewis lung cancer volume. (G) Kaplan–Meier curves for an illustration of the survival periods of ischemic insult combined with Lewis Lung cancer xenograft mice model. Data (B)–(E) represent mean ± SEM, n = 8–10 mice per group. $^{*}p < 0.05$, $^{**}p < 0.01$ and $^{***}p < 0.001$ compared with curcumin free group (control).

stimulate collateral blood-flow recovery in response to ischemic conditions and the high dose group recovers faster than the low dose one.

Meanwhile, we also observed the influence of curcumin on LLC growth. Fig. 1C showed that curcumin significantly impaired lung cancer growth dose-dependently by day 22 ($p < 0.05$). Meanwhile, lung net weight (Fig. 1D), number of pulmonary metastases (Fig. 1E) and primary tumor volume (Fig. 1F) also dramatically decreased with curcumin administration. In addition, change of survival rate was effectively enhanced by curcumin, as evidenced by a 29% increase (300 mg/kg curcumin group) over that of the vehicle on day 21 (Fig. 1G). Thus, considered together, this data indicates the inhibitory role of curcumin on lung cancer in ischemia and LLC bearing mice.

3.2. Curcumin increases ischemic muscle microvessel density, but retards lung cancer angiogenesis

To assess whether curcumin would stimulate or inhibit angiogenesis in the ischemia and lung cancer mouse model, freshly resected cancer tissues and ischemic muscles were examined using CD31 staining. Oral administration of curcumin at 300 mg/kg/day significantly

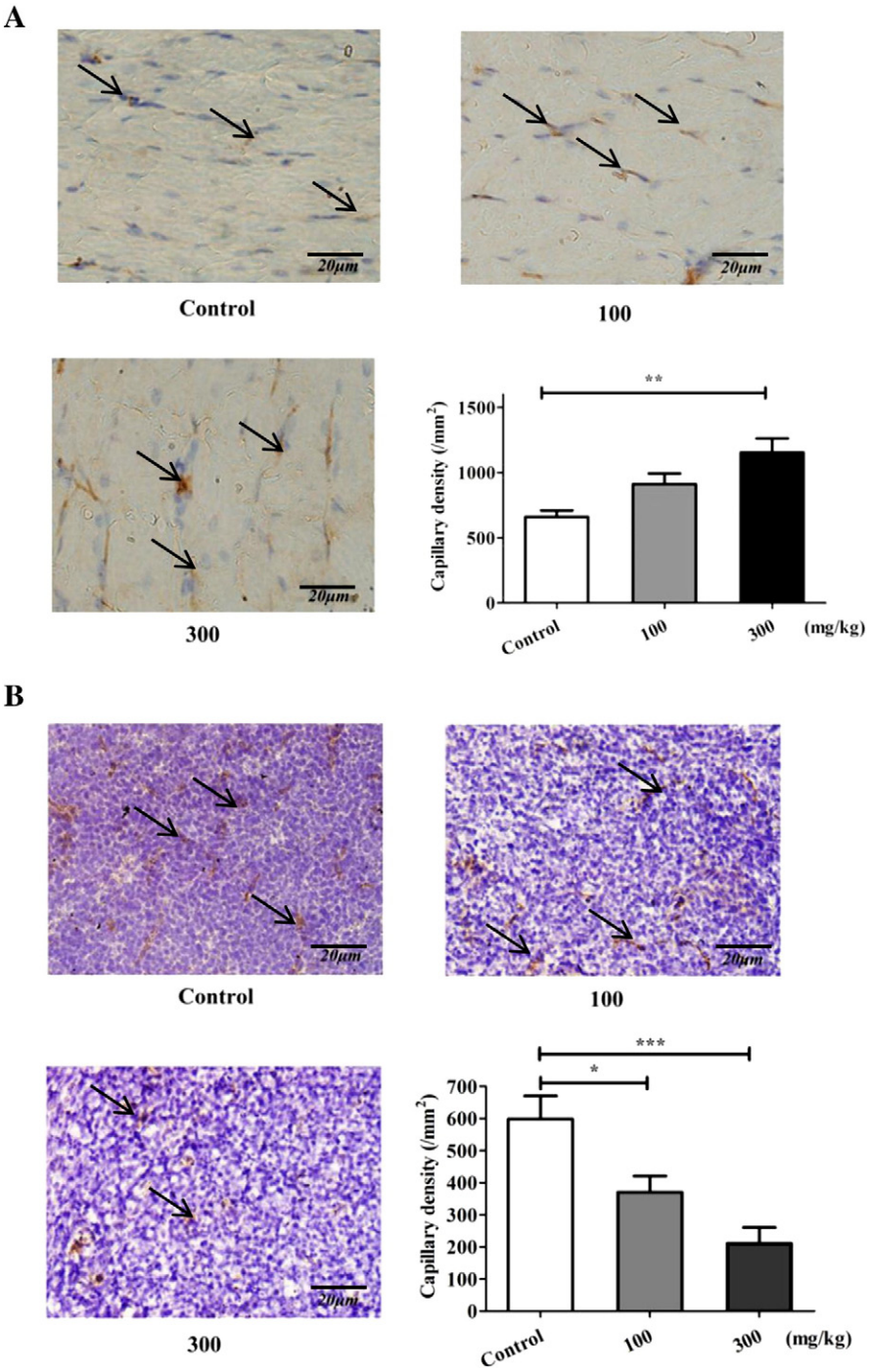

Fig. 2. Representative CD31 immunohistochemistry images for capillary density (arrow). (A) Images of immunohistological assay and statistical result of CD31 expression in ischemic muscle tissues. (B) Images of immunohistological assay and statistical result of CD31 expression in primary Lewis lung cancer tissues. Data represent mean ± SEM, n = 6. $^{*}p < 0.05$, $^{**}p < 0.01$ and $^{***}p < 0.001$ compared with the curcumin free group (control). Original magnification ×250 (scale bars: 20 μm).

increased the number of blood vessels in ischemic limb, as evidenced by the positive area in Fig. 2A. In contrast, curcumin impaired capillary regeneration in cancer tissues, as indicated by a 74.8% decrease (Fig. 2B). In brief, these observations are compatible with the notion that curcumin administration can stimulate post-ischemic revascularization and inhibit angiogenesis against primary LLC synchronously.

3.3. HUVEC and CAM exhibit differential sensitivities to curcumin

To investigate the *in vitro* angiogenic responses, we treated HUVEC with increasing concentrations of curcumin, from 0.01 to 30 μM for 24 h. Striking variations on HUVEC were observed as shown in Fig. 3A and B. In the presence of concentrations from 0.1 to 0.3 μM, capillary-like tube length concentration-dependently increased after curcumin treatment. Whereas, curcumin reversed these alternations dramatically within the scope of 3 to 10 μM.

In order to further elaborate neovascularization with or without curcumin treatment, we additionally performed chicken CAM assays *in vivo*. Fig. 3C and D shows the digitized representations of emblematical CAM treated for 72 h with curcumin. Results indicated the number of small blood vessels increased significantly within the dosage range of 1 to 3 μM. In contrast, in the presence of 10 to 30 μM, a dose-specific suppression of blood vessel regeneration occurred. In short, our results reveal the Janus face of curcumin on tube formulation and neovascularization as a function of dose.

3.4. Curcumin negatively or positively regulates the HIF1α/mTOR/VEGF/VEGFR cascade in ischemic muscle and primary LLC tissues, respectively

We next sought to address the specific signaling pathways affected by curcumin in ischemic muscles and LLC xenograft tissues in the mouse model simultaneously. Our model for the construction of the primary GRNs was based on the utilization of interaction from target prediction. As of June 2012, the list contained 3,494 and 7,064 nodes in ischemia and lung cancer, respectively (Raw data were appended in Additional file). Starting from the gene association network based on PubMed, Agilent LitSearch tool created two biologically relevant projections (Fig. 4A and B). After intersecting with Network Merge plugin, the overlapped genes entangled in ischemia and lung cancer were clustered by MCODE algorithm (Fig. 4C).

Genes in disease-associated communities always share similarities in which they are inclined to connect. This dense clique within a network is regarded as GRNs. As shown in Fig. 4D to G, with the higher degree of gene regulation, we inferred the underlying biological

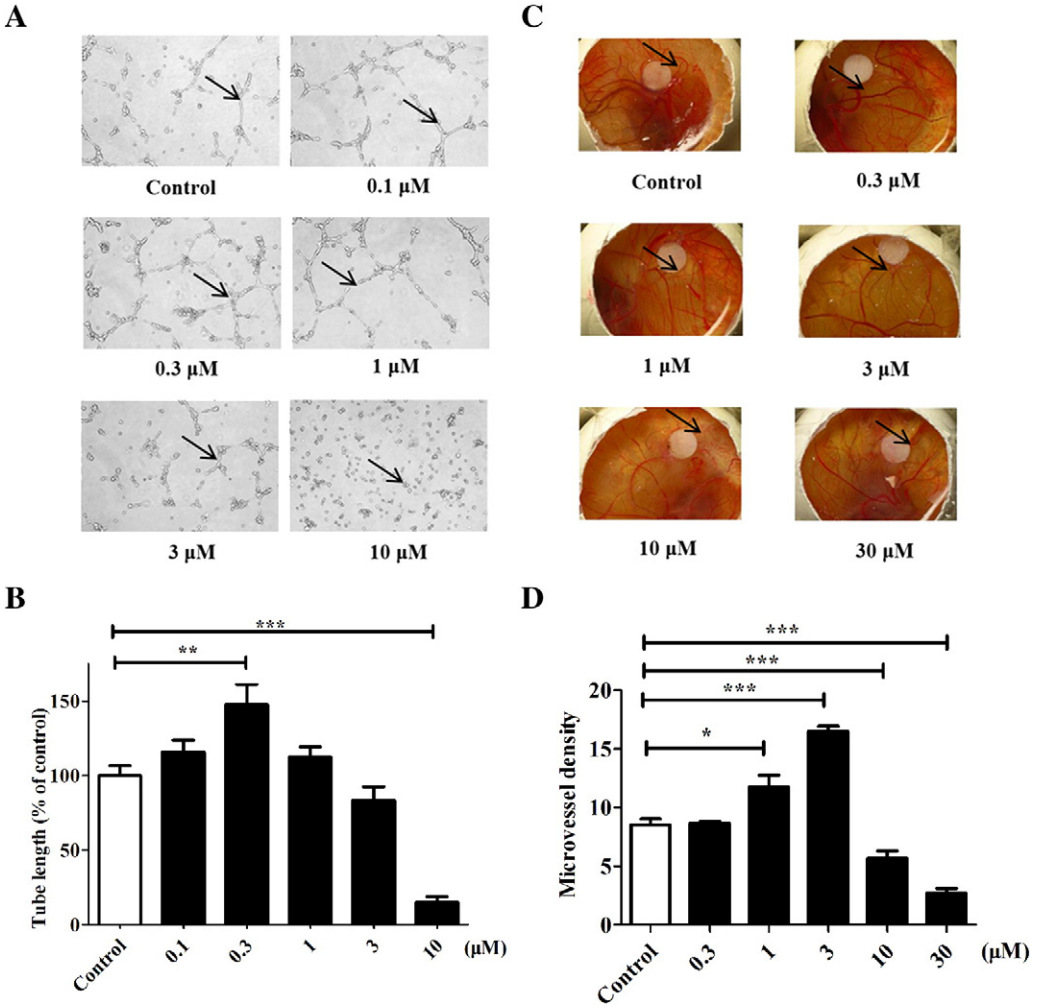

Fig. 3. Effect of curcumin on HUVEC tube formation and CAM neovascularization. (A) Capillary-like tube formulation (arrow) assay of curcumin. (B) Statistical results of tube formulation assay on HUVEC. (C) CAM assay of curcumin on neovascularization (arrow). (D) Statistical results of tube formulation assay on HUVEC. Data (B) and (D) represent mean ± SEM, n = 3. $^{*}p < 0.05$, $^{**}p < 0.01$ and $^{***}p < 0.001$ compared with the curcumin free group (control). Original magnification ×400.

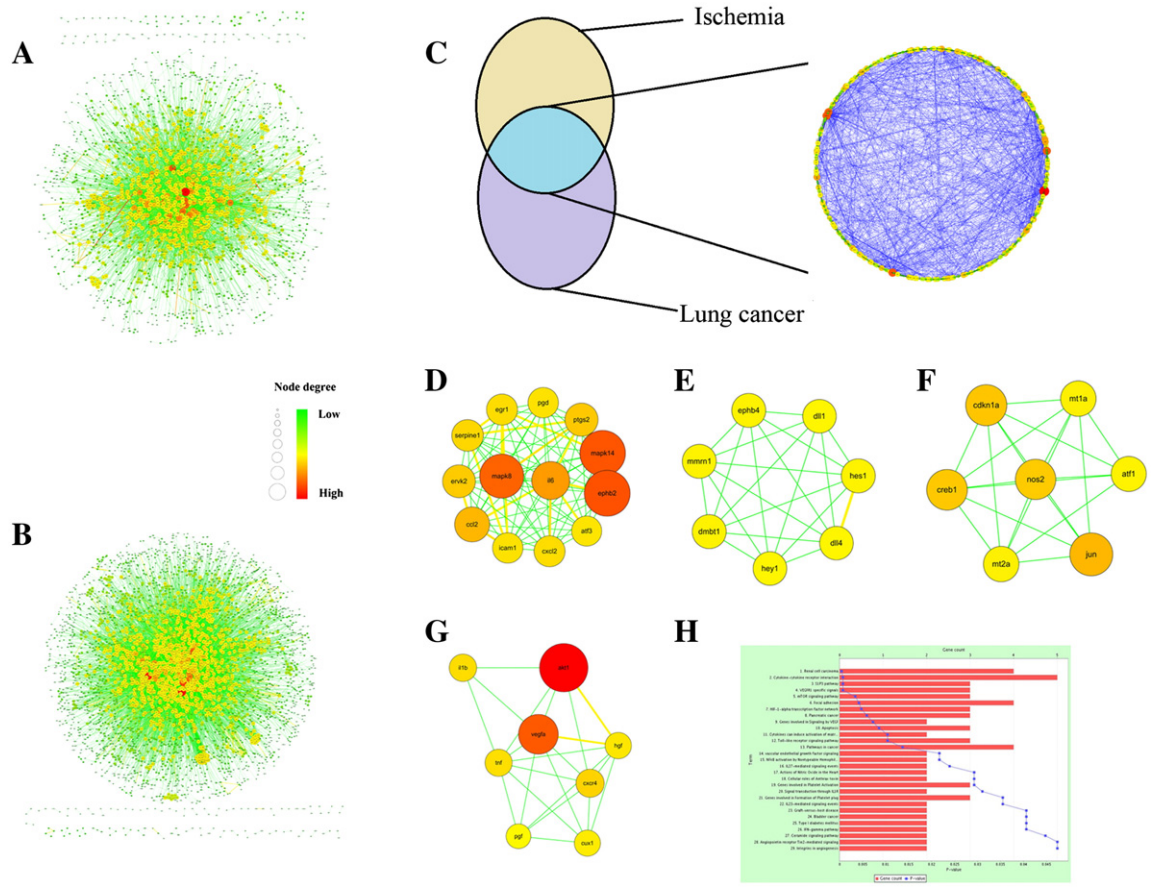

Fig. 4. Visualization of human disease-gene interaction networks (Force-Directed Layout) and pathway enrichment analysis result. (A) Ischemia network contains 1,836 nodes and 8,286 edges. (B) Lung cancer network contains 3,171 nodes and 17,439 edges. (C) The overlapped genes between ischemia and lung cancer data (Grid Layout). Intersections of gene sets comprised 1,234 nodes and 1,488 edges. (D)–(G) Gene regulatory networks (GRNs) obtain from the overlapped genes. Gene-sets fail to pass the enrichment cluster score threshold of 2.0 are not shown. Each node (represents as a circle) matches to a gene, and edges represent interactions of nodes: red represents high degree connectivity, whereas green represents low degree connectivity. The size of each node is proportionate to the degree. (H) Pathway enrichment analysis results of the overlapped GRNs based on ToppFun (*FDR* < 0.05).

pathways driven by these prominent GRNs between those two dysfunctions. As presented in Fig. 4H, the enriched signaling pathways in multiple categories were selected with a *FDR* threshold less than 0.05, which indicated cytokine–cytokine receptor interaction, S1P3 pathway, VEGFR specific signals, mTOR signaling pathway, Focal adhesion, HIF1α transcription factor network and genes involved in signaling by VEGF might play decisive roles in ischemia and lung cancer simultaneously.

To explain the dual phenotype obtained from the *in vivo* and *in vitro* findings, and increase our understanding of the underlying mechanisms, we conducted a series of Western blot, real-time PCR and ELISA analysis with or without curcumin treatment. Our data revealed that curcumin increased HIF1α, p-mTOR/mTOR, VEGF and VEGFR in ischemic muscles, but reversed these alternations, as indicated by 50% to 100% decrease in the primary LLC tissues (Fig. 5). Thus, consistent with the *in silico* prediction, our data strongly suggest that the dual angiogenic effects of curcumin in ischemic insult and primary lung cancer are mediated by the HIF1α/mTOR/VEGF/VEGFR cascade but in the opposite fashion.

3.5. α1-AT is a serum biomarker for ischemia and LLC mice model

In mice exposed to 300 mg/kg curcumin, two differently expressed proteins regulated by curcumin were detected by 2-DE (Fig. 6A). As presented in Fig. 6B to D, α1-AT (spot 1) and transthyretin (TTR, spot 2) were identified via sequence analysis, using ESI-Q-TOP-MS and database retrieval. Since an imbalance of NE and α1-AT was a risk factor for malignant initiation and progression, the down-regulation of α1-AT in mouse serum was of interest and deserved further investigation [33,34].

3.6. Curcumin increases α1-AT production, but blocks NE release in LLC tissues

Aberrant expression of NE is associated with tumor initiation [35]. In mice with ischemia and lung cancer, obvious expression of NE was observed in primary lung cancer tissues. Curcumin dramatically reversed the inflammatory alternations seen for α1-AT and NE in LLC tissues (Fig. 6E to G). In fact, α1-AT secretion was remarkably increased after curcumin treatment at both low and high doses. Of note, neither of the two proteins could be detected in ischemic muscles with or without curcumin treatment (data not shown). Thus, our data suggest that the pernicious effects of NE on lung cancer angiogenesis are abolished by treatment with curcumin.

3.7. IRS-1 protein is upregulated in the primary lung cancer tissues after curcumin treatment

It has been documented that NE can promote the degradation of insulin receptor substrate-1 (IRS-1) protein and accelerate lung cancer growth [36], as IRS-1 is a key regulator of PI3K within various malignancies. In the present study, we discovered that curcumin significantly promoted IRS-1 expression in the lung cancer tissues compared to the

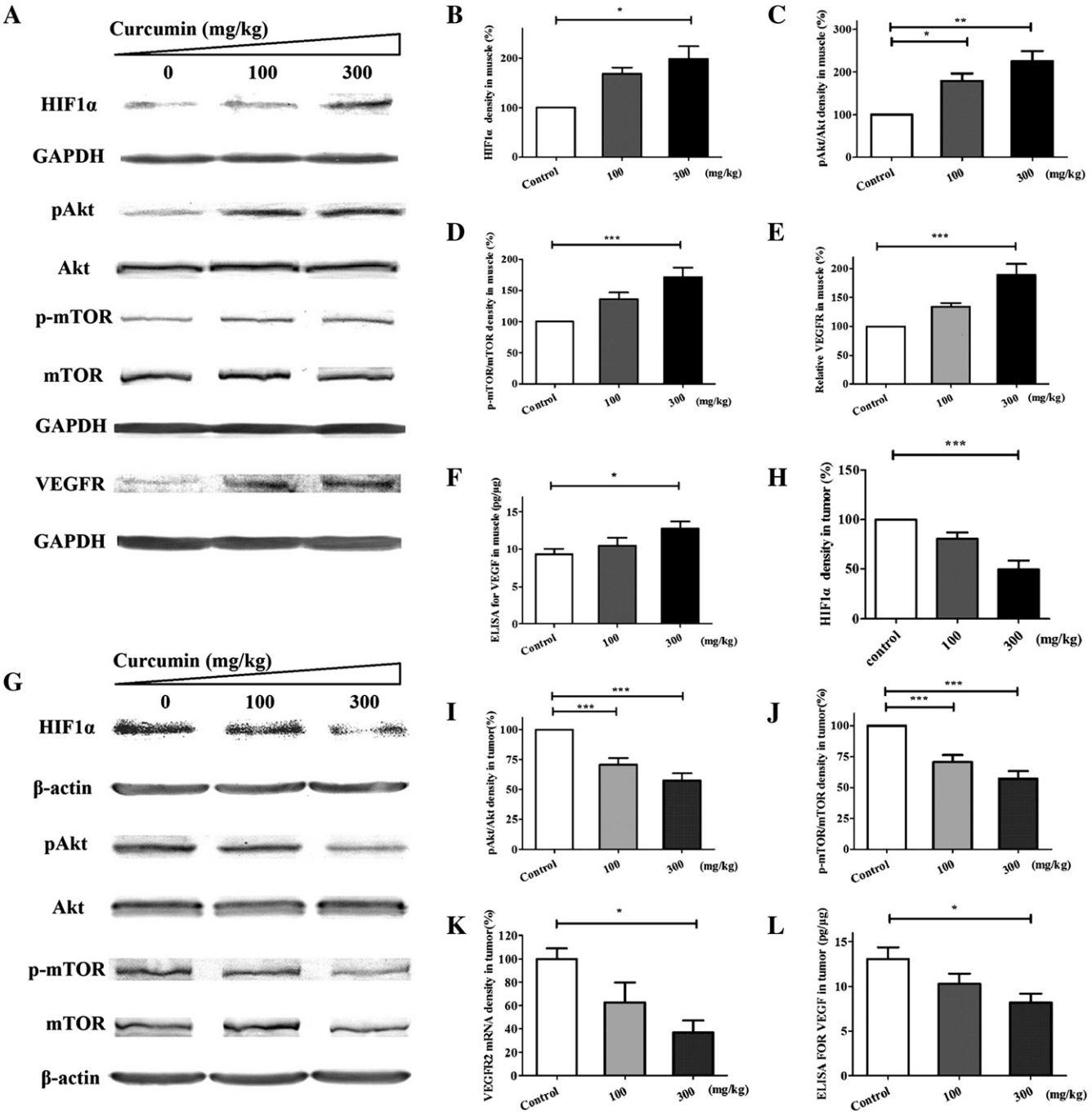

Fig. 5. Curcumin differently regulated VEGFR/mTOR/HIF1α/VEGF cascade in ischemia and LLC model. (A) Images of Western blot analysis of HIF1α, pAkt/Akt, p-mTOR/mTOR and VEGFR expression levels in the ischemic muscles. (B)–(E) Statistical analysis of Western blot for HIF1α, pAkt: Akt ratio, p-mTOR: mTOR ratio and VEGFR in the ischemic muscles. (F) Statistical analysis of ELISA for VEGF in the ischemic muscles. (G) Images of Western blot analysis of HIF1α, pAkt/Akt and p-mTOR/mTOR expression levels in the primary Lewis lung cancer tissues. (H)–(J) Statistical analysis of Western blot for HIF1α, pAkt: Akt ratio and p-mTOR: mTOR ratio in the primary Lewis lung cancer tissues. (K) Statistical analysis of quantitative real-time PCR for VEGFR mRNA in the primary Lewis lung cancer tissues. (L) Statistical analysis of ELISA for VEGF in the primary Lewis lung cancer tissues. Data represent mean ± SEM, n = 6. $^{*}p < 0.05$, $^{**}p < 0.01$ and $^{***}p < 0.001$ compared with the curcumin free group (control).

vehicle group (Fig. 6E and H). Overall, our results indicate that curcumin is able to promote IRS-1 expression in the primary lung cancer tissues via downregulation of NE.

3.8. NE is identified as a direct protein-target for curcumin

To investigate the interaction of NE and curcumin, specific binding of curcumin to hNE was conducted by molecular dynamics study and SPR analysis. The *in silico* drug target docking modeling analysis indicated that curcumin could directly cage into the binding pocket of NE (Fig. 7A to C) with 27.4099 kcal/mol in its best binding pose. As shown in Fig. 7B, both ARG178 and ARG217 play decisive roles in H-bond formation, which contributed to stabilizing the complex of NE and curcumin. The RMSD reference of curcumin, plotted in Fig. 7D, showed that the interaction of the receptor-ligand complex reached the equilibrium state after 7 s. A similar situation could be observed in the interaction analysis between the O of curcumin and HH in the amino residue of Arg178 and ARG217 in NE (Fig. 7E and F). All the

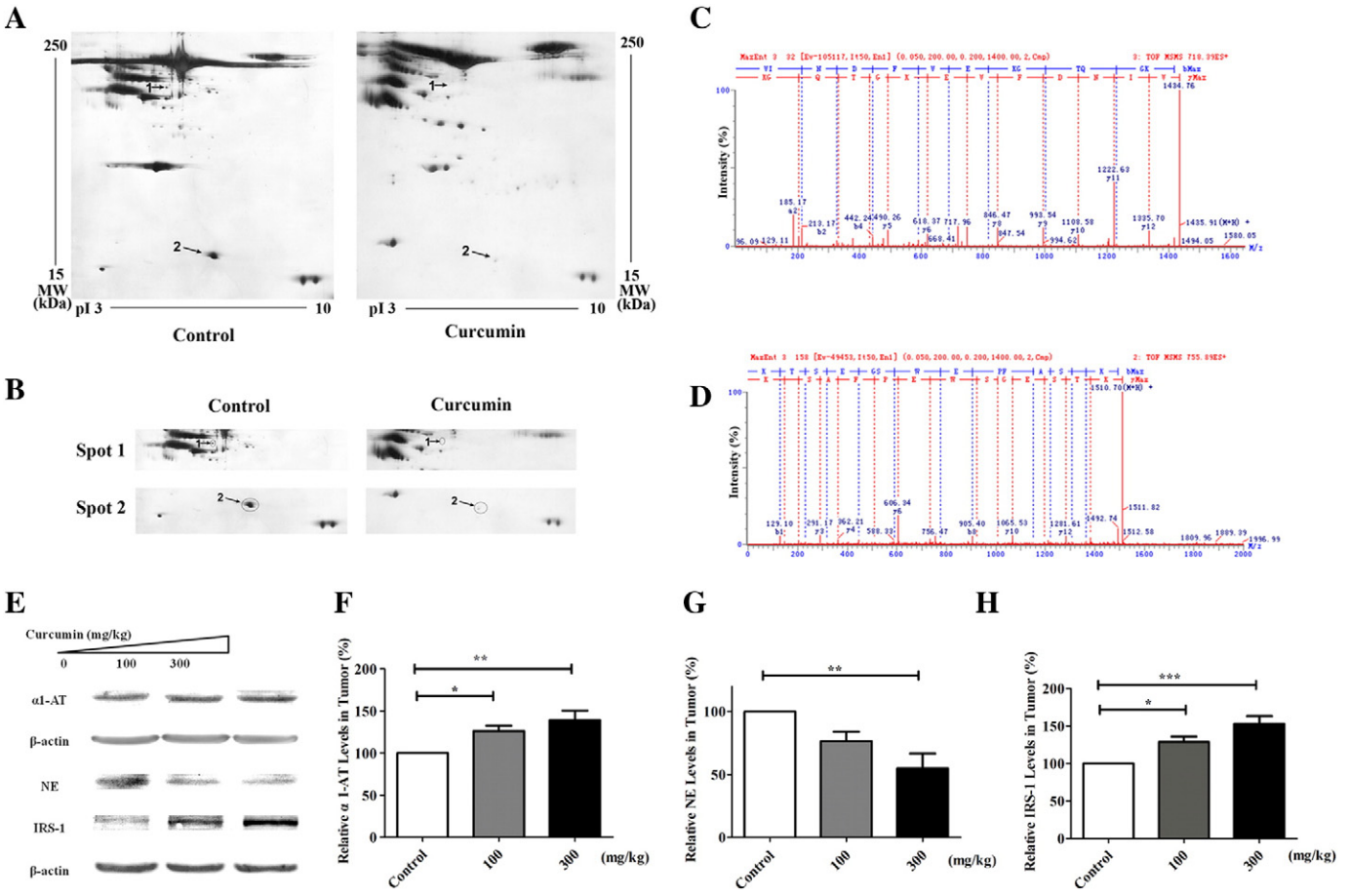

Fig. 6. Proteomics identification of proteins differentially expressed in mice serum obtained from ischemic insult collaborated with lung cancer mice model before and after curcumin treatment. (A) Two-dimensional gel electrophoresis (2-DE) images of serum proteins in the presence of curcumin (300 mg/kg/day) or vehicle. Gel pair is the representative images of six replicate gels obtained from three independent experiments. Differentially expressed spots are pointed out by the arrows. (B) Expanded regions of the differentially expressed protein spots (circles). (C) Result of ESI-Q-TOP-MS analysis of α1-antitrypsin (α1-AT, as spot 1). (D) Result of ESI-Q-TOP-MS analysis of transthyretin (TTR, as spot 2). (E) Images of Western blot analysis of α1-AT, NE and IRS-1protein expression levels in the primary Lewis lung cancer tissues. (F) Statistical analysis of Western blot for α1-AT in the primary Lewis lung cancer tissues. (G) Statistical analysis of Western blot for NE in the primary Lewis lung cancer tissues. (H) Statistical analysis of Western blot for IRS-1 in the primary Lewis lung cancer tissues. Data (F)–(H) represent mean ± SEM, n = 6. $^{*}p < 0.05$, $^{**}p < 0.01$ and $^{***}p < 0.001$compared with the curcumin free group (control).

interactions were formed at the beginning of the calculation (5 s). These results suggest that these two residues of the catalytic site can stabilize the interaction between curcumin and NE.

Further, we additionally investigated the binding affinity of curcumin towards NE based on SPR. As presented in Fig. 7G, response units (RU) values significantly increased with the incremental curcumin doses from 7.5 to 120 μM, indicating curcumin could directly bind to NE in a concentration-dependent manner. The association (k_a) and dissociation (k_d) rate constants of curcumin binding to the immobilized NE on a CM_5 chip were 275 M^{-1} s^{-1} and 8.73×10^{-3} s^{-1}, respectively. The equilibrium dissociation constant ($K_D = k_d/k_a$) was 3.17×10^{-5} M. These results mentioned above confirm NE is a direct target for curcumin.

4. Discussion

In the present study, we discovered that curcumin accelerated blood flow restoration and promoted post-ischemic revascularization. In contrast, NE secretion benefited lung cancer progression, but this alternation was reversed by curcumin. Thus, the present results demonstrate the opposite effect of curcumin on angiogenesis in ischemia and LLC growth in a simultaneous mouse model.

According to the recent publications, the availability of proteomics approach has been widely utilized in the discovery of disease biomarkers [37–39]. To better elucidate the opposite angiogenesis action mediated by curcumin *in vivo*, we first performed 2-DE in mouse serum and discovered that oral administration of curcumin decreased α1-AT secretion. Other investigations have demonstrated α1-AT was decreased remarkably in a variety of malignancies, especially lung cancer [40–43]. Imbalance of NE and α1-AT was considered as a risk factor for lung cancer progression. A recent work reported that NE and α1-AT were involved in lung cancer proliferation. It was found that *in vitro* hNE treatment of human A549 and Calu-3 lung cancer cells mimicked cell proliferation as seen in the LLC xenograft mouse model. In addition, curcumin decreased endogenous and/or exogenous NE production, which in turn, retarded tumor growth in primary lung cancer tissues [44]. Thus, consistent with this previous report, our data further confirm NE can stimulate lung cancer angiogenesis and curcumin can reverse this undesirable action mediated by NE.

Inference GRNs using the target prediction method deepened our understanding genes associated with illnesses. To further elucidate the underlying mechanisms mediated by curcumin, we enriched the signaling pathways involved in ischemia and lung cancer. Among them, VEGFR specific signals, mTOR signaling pathway, HIF1α transcription factor network and genes involved in signaling by VEGF have been shown to be highly associated with ischemic insult and lung cancer synchronously. These findings are consistent with the incremental evidences for the involvement of HIF1α, mTOR, VEGF and VEGFR in ischemia and lung cancer [45].

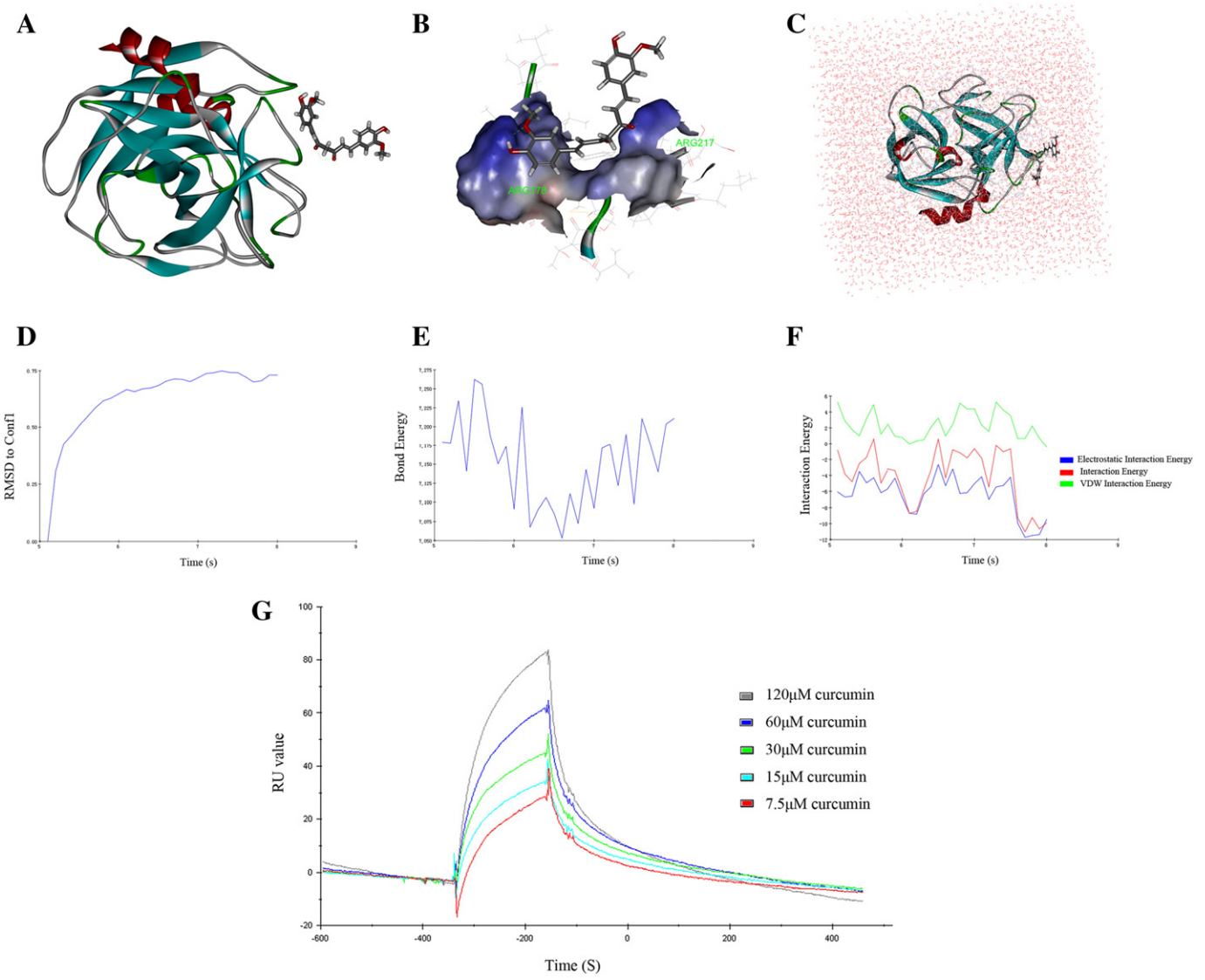

Fig. 7. Protein-ligand interaction, molecular dynamics and binding affinity studies of NE and curcumin. (A) Interaction models of NE and curcumin in the best docking pose. (B) Detailed interaction modes of NE and curcumin in the best docking pose. (C) Model of NE and curcumin in solvent. (D) Drug positional RMSD. (E) Interaction bond energy of amino residue group between NE and curcumin. (F) Interaction energy of amino residue group between NE and curcumin through all the molecular dynamics. Curcumin is in the stick representation, while the residues of NE are presented by solid style in the line representation. Hydrogen bonds are depicted by green dotted lines. Water is depicted by pink. C, H, and O are colored in gray, white, and red, respectively. (G) Real time binding affinity measurements of curcumin using Biacore 3000. Representative sensorgrams are obtained from the injections of curcumin at different concentrations of 120, 60, 30, 15, and 7.5 μM (curve from top to bottom) over the immobilized NE surface on the CM_5 chip.

As an indispensable vascular remodeling factor which bound heparin and acted via their affinity transmembrane receptors VEGFR1 and VEGFR2, VEGF is a fundamental molecular regulator of angiogenesis [46]. Studies have reported that there was a strong local production of VEGF in lungs of patients with lung cancer and the up-regulation of VEGF has been found in highly-malignant cancer [47]. As mentioned, various anti-angiogenic avenues to block VEGF in cancer are under development [48]. Bevacizumab (Avastin), a VEGF-neutralizing antibody, has been recommended and approved by the US Food and Drug Administration for several metastatic cancers. Besides, treatment with other VEGF inhibitors also prolonged the survival of cancer patients as summarized by Carmeliet et al. [49]. The clinical use of VEGF blockade for anti-angiogenic therapy, however, is still not optimistic owing to its cytotoxicity and poor selectivity [50]. In this present study, we examined the concentrations of VEGF in lung cancer and ischemic muscles and discovered VEGF concentrations distributed in lung cancer were much higher than the ischemic tissues. As a natural product with great safety and low toxicity, curcumin could efficiently inhibit vascularization via downregulation of VEGF in lung cancer. With regard to ischemic tissues, VEGF contents were significantly increased, resulting in pro-angiogenesis. Although the clinical significance of curcumin for angiogenesis is controversial, the beneficial effects could be seen in the ischemia and lung cancer mice model.

In response to VEGF, activation of VEGFR contributes to stimulating angiogenesis. Thus, further studies on VEGF/VEGFR axis facilitate our understanding of the physiological process involved in ischemia and allow us to put forward a proposal to retard angiogenesis in lung cancer. Emerging evidences indicate that VEGF exerts protective effects against acute myocardial ischemia through stimulation of VEGFR2 [51]. The mechanism by which curcumin mediates ischemic angiogenesis remains unknown. In our study, the upregulation of VEGFR2 in the ischemic tissues was corroborated by Western blot after curcumin treatment. However, there was no significant alternation of VEGFR2 protein level in lung cancer in the presence and absence of curcumin. The significant

decrease of VEGFR mRNA did not cohere with the recent findings in pancreatic cancer cell, which indicated that the anti-proliferative effect of curcumin took effect via downregulation of VEGFR protein expression [52]. This difference may be contributed to the variation of cancer cell type.

Recently, Sidhu et al. [53] reported that curcumin could accelerate wound healing in diabetic mice after topical application by repairing collagen, hexosamine and damaged DNA. Meanwhile, without serum, curcumin induced EC differentiation, increased capillary vessel density in CAM, and promoted morphological alterations of pro-angiogenic phenotype on HUVEC via elevation of CD31, E-selectin, VEGF and VEGFR2 production. In contrast, under serum stimulated conditions, curcumin revealed an anti-angiogenic effect on EC, CAM and HUVEC through negative control of angiogenic factors. It was confirmed that curcumin treatment could distinguish between normal and abnormal cells, and create recognizable angiogenesis in different cellular microenvironments [54]. Consistent with the conclusion mentioned above, in the present study, our data *in vitro* show that curcumin reveals opposite angiogenic effects on HUVEC and chicken CAM as a function of dose.

Interestingly, biphasic dose responses of curcumin on revascularization have been frequently observed i.e. low levels of curcumin have an angiogenesis stimulating effect while higher doses inhibit angiogenesis [55]. Thaloor et al. [56] discovered that curcumin revealed a pro-angiogenic effect at a low therapeutic concentration (20 mg/kg/day), whereas it suppressed tumor progression in the high dose groups (100 to 300 mg/kg/day) in C57BL/6 mice [44]. Whether stimulatory and/or inhibitory responsiveness would occur in a combined ischemic insult and lung cancer model to curcumin, as described in low and high doses *in vivo* studies, was not known. Interestingly, our present study discloses that curcumin can retard tumor growth by decreasing NE secretion. Meanwhile, it also reveals a dual angiogenic outcome in a simultaneous mouse model with ischemia and LLC. Inflammation is highly associated with cancer initiation and progression. Molecular mechanisms about how curcumin gives rise to opposite angiogenic effects in such a murine mouse model might be attributed to the inflammatory activity of NE in the microenvironment of lung cancer. Briefly, curcumin distributed in ischemic hind limb promotes post-ischemic neovascularization via activation of the HIF1α/mTOR/VEGF/VEGFR cascade [57]. In contrast, in the LLC tissues, curcumin reveals an inhibitory phenotype by directly binding to NE causing a disequilibrium between α1-AT and NE, which subsequently gives rise to the anti-tumorigenic effect in the primary lung cancer tissues. Dual angiogenic mechanisms evoked by curcumin are presented in a simplified model (Fig. 8).

In summary, the main findings of the present experiment were that: (1) curcumin caused opposite angiogenic effects in an ischemic insult model and LLC mouse tumor model in the same mouse; (2) Janus faced angiogenic effects mediated by curcumin in this model relied on the HIF1α/mTOR/VEGF/VEGFR cascade; (3) curcumin could reverse the angiogenic effect mediated by NE in lung cancer tissues; and (4)

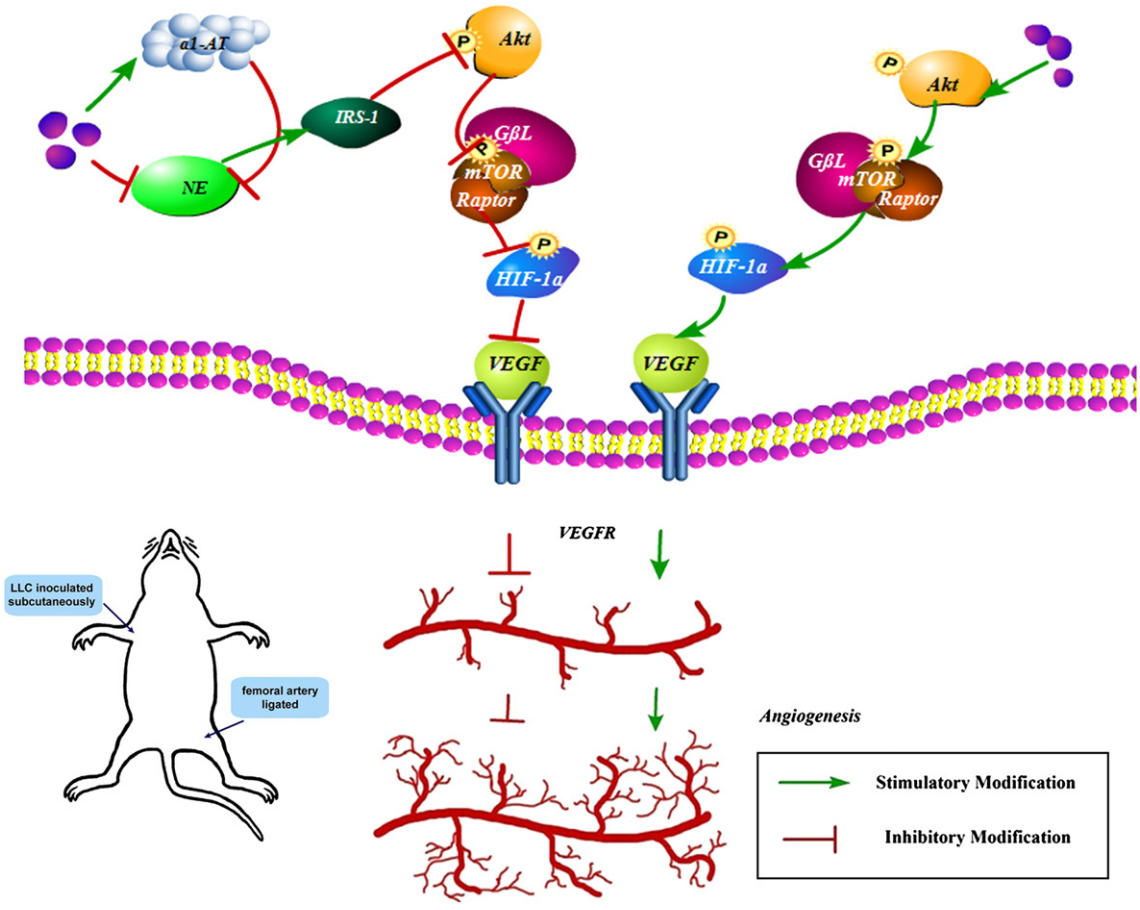

Fig. 8. Schematic diagram of curcumin regulatory pathway against ischemic insult and Lewis lung cancer synchronously. Angiogenesis of curcumin against ischemic hind limb was hypothesized to occur through the binding and reacting with VEGFR specific signaling pathway, mTOR pathway, HIF1α transcription factor network and genes involved in signaling by VEGF. The diagram shows that curcumin promotes the expression of hub-proteins, resulting in vascular regeneration in response to ischemic insult. Contrarily, curcumin in lung cancer reduces endogenous NE secretion and rebalanced the equilibriums of α1-AT and NE in lung cancer tissues via direct interaction with NE. This action subsequently down-regulates the expression of relevant proteins in the HIF1α/mTOR/VEGF/VEGFR cascade and inhibits LLC progression of the ischemia and Lewis lung carcinoma mice model.

the favorable angiogenic effects of curcumin could in part benefit individuals who suffer from both ischemic disorders and lung cancer.

Conflict of interest statement

The authors declare that they have no competing interests.

Acknowledgements

We would like to thank Dr Liangren Zhang of the State Key Laboratory of Natural and Biomimetic Drugs of Peking University Health Science Center for guiding the molecular docking and dynamics studies. This work was supported by the National Natural Science Foundation of China (No. 91129727, 81020108031, 30973558, 81270049, 81373405) and Research Fund from Ministry of Education of China (111 Projects No. B07001). The funders had no role in study design, data collection and analysis, decision to publish, or in the preparation of the manuscript.

Appendix A

List of the significant genetic genes involved in ischemia and lung cancer screened from OMIM, GAD and GeneCard databases.

References

[1] G. Zerbini, M. Lorenzi, A. Palini, Tumor angiogenesis, N. Engl. J. Med. 359 (2008) 763–764.
[2] E. Duh, L.P. Aiello, Vascular endothelial growth factor and diabetes: the agonist versus antagonist paradox, Diabetes 48 (1999) 1899–1906.
[3] B. Witzenbichler, T. Asahara, T. Murohara, M. Silver, I. Spyridopoulos, M. Magner, N. Principe, M. Kearney, J.S. Hu, J.M. Isner, Vascular endothelial growth factor-C (VEGF-C/VEGF-2) promotes angiogenesis in the setting of tissue ischemia, Am. J. Pathol. 153 (1998) 381–394.
[4] Z.G. Zhang, L. Zhang, Q. Jiang, R. Zhang, K. Davies, C. Powers, N. Bruggen, M. Chopp, VEGF enhances angiogenesis and promotes blood–brain barrier leakage in the ischemic brain, J. Clin. Invest. 106 (2000) 829–838.
[5] D. Lambrechts, E. Storkebaum, M. Morimoto, J. Del-Favero, F. Desmet, S.L. Marklund, S. Wyns, V. Thijs, J. Andersson, I. van Marion, A. Al-Chalabi, S. Bornes, R. Musson, V. Hansen, L. Beckman, R. Adolfsson, H.S. Pall, H. Prats, S. Vermeire, P. Rutgeerts, S. Katayama, T. Awata, N. Leigh, L. Lang-Lazdunski, M. Dewerchin, C. Shaw, L. Moons, R. Vlietinck, K.E. Morrison, W. Robberecht, C. Van Broeckhoven, D. Collen, P.M. Andersen, P. Carmeliet, VEGF is a modifier of amyotrophic lateral sclerosis in mice and humans and protects motoneurons against ischemic death, Nat. Genet. 34 (2003) 383–394.
[6] P. Carmeliet, Angiogenesis in health and disease, Nat. Med. 9 (2003) 653–660.
[7] A. Rapisarda, G. Melillo, Role of the VEGF/VEGFR axis in cancer biology and therapy, Adv. Cancer Res. 114 (2012) 237–267.
[8] H.S. Kim, Do not put too much value on conventional medicines, J. Ethnopharmacol. 100 (2005) 37–39.
[9] G. Bar-Sela, R. Epelbaum, M. Schaffer, Curcumin as an anti-cancer agent: review of the gap between basic and clinical applications, Curr. Med. Chem. 17 (2010) 190–197.
[10] C. Rozzo, M. Fanciulli, C. Fraumene, A. Corrias, T. Cubeddu, I. Sassu, S. Cossu, V. Nieddu, G. Galleri, E. Azara, M.A. Dettori, D. Fabbri, G. Palmieri, M. Pisano, Molecular changes induced by the curcumin analogue D6 in human melanoma cells, Mol. Cancer 12 (2013) 37.
[11] A.S. Strimpakos, R.A. Sharma, Curcumin: preventive and therapeutic properties in laboratory studies and clinical trials, Antioxid. Redox Signal. 10 (2008) 511–545.
[12] S. Miriyala, M. Panchatcharam, P. Rengarajulu, Cardioprotective effects of curcumin, Adv. Exp. Med. Biol. 595 (2007) 359–377.
[13] G. Srivastava, J.L. Mehta, Currying the heart: curcumin and cardioprotection, J. Cardiovasc. Pharmacol. Ther. 14 (2009) 22–27.
[14] Z.J. Sun, G. Chen, W. Zhang, X. Hu, Y. Liu, Q. Zhou, L.X. Zhu, Y.F. Zhao, Curcumin dually inhibits both mammalian target of rapamycin and nuclear factor-kappaB pathways through a crossed phosphatidylinositol 3-kinase/Akt/IkappaB kinase complex signaling axis in adenoid cystic carcinoma, Mol. Pharmacol. 79 (2011) 106–118.
[15] S.S. Lin, K.C. Lai, S.C. Hsu, J.S. Yang, C.L. Kuo, J.P. Lin, Y.S. Ma, C.C. Wu, J.G. Chung, Curcumin inhibits the migration and invasion of human A549 lung cancer cells through the inhibition of matrix metalloproteinase-2 and −9 and vascular endothelial growth factor (VEGF), Cancer Lett. 285 (2009) 127–133.
[16] D.G. Binion, M.F. Otterson, P. Rafiee, Curcumin inhibits VEGF-mediated angiogenesis in human intestinal microvascular endothelial cells through COX-2 and MAPK inhibition, Gut 57 (2008) 1509–1517.
[17] Y.T. Tung, H.L. Chen, C.W. Lai, C.J. Shen, Y.W. Lai, C.M. Chen, Curcumin reduces pulmonary tumorigenesis in vascular endothelial growth factor (VEGF)-overexpressing transgenic mice, Mol. Nutr. Food Res. 55 (2011) 1036–1043.
[18] G. Chakraborty, S. Jain, S. Kale, R. Raja, S. Kumar, R. Mishra, G.C. Kundu, Curcumin suppresses breast tumor angiogenesis by abrogating osteopontin-induced VEGF expression, Mol. Med. Rep. 1 (2008) 641–646.
[19] G. Hansen, H. Gielen-Haertwig, P. Reinemer, D. Schomburg, A. Harrenga, K. Niefind, Unexpected active-site flexibility in the structure of human neutrophil elastase in complex with a new dihydropyrimidone inhibitor, J. Mol. Biol. 409 (2011) 681–691.
[20] P. Shamamian, J.D. Schwartz, B.J. Pocock, S. Monea, D. Whiting, S.G. Marcus, P. Mignatti, Activation of progelatinase A (MMP-2) by neutrophil elastase, cathepsin G, and proteinase-3: a role for inflammatory cells in tumor invasion and angiogenesis, J. Cell. Physiol. 189 (2001) 197–206.
[21] D.H. Perlmutter, Alpha-1-antitrypsin deficiency: biochemistry and clinical manifestations, Ann. Med. 28 (1996) 385–394.
[22] R. Mohan, J. Sivak, P. Ashton, L.A. Russo, B.Q. Pham, N. Kasahara, M.B. Raizman, M.E. Fini, Curcuminoids inhibit the angiogenic response stimulated by fibroblast growth factor-2, including expression of matrix metalloproteinase gelatinase B, J. Biol. Chem. 275 (2000) 10405–10412.
[23] P. Yoysungnoen, P. Wirachwong, P. Bhattarakosol, H. Niimi, S. Patumraj, Effects of curcumin on tumor angiogenesis and biomarkers, COX-2 and VEGF, in hepatocellular carcinoma cell-implanted nude mice, Clin. Hemorheol. Microcirc. 34 (2006) 109–115.
[24] S. Brandon, Ethics, economics and science, J. R. Soc. Med. 84 (1991) 575–577.
[25] M. Sata, H. Nishimatsu, J. Osuga, K. Tanaka, N. Ishizaka, S. Ishibashi, Y. Hirata, R. Nagai, Statins augment collateral growth in response to ischemia but they do not promote cancer and atherosclerosis, Hypertension 43 (2004) 1214–1220.
[26] Y. Yamashita-Kashima, K. Fujimoto-Ouchi, K. Yorozu, M. Kurasawa, M. Yanagisawa, H. Yasuno, K. Mori, Biomarkers for antitumor activity of bevacizumab in gastric cancer models, BMC Cancer 12 (2012) 37.
[27] K. Kunimasa, T. Ohta, H. Tani, E. Kato, R. Eguchi, K. Kaji, K. Ikeda, H. Mori, M. Mori, T. Tatefuji, Y. Yamori, Resveratrol derivative-rich Melinjo (*Gnetum gnemon* L.) seed extract suppresses multiple angiogenesis-related endothelial cell functions and tumor angiogenesis, Mol. Nutr. Food Res. 55 (2011) 1730–1734.
[28] D. Ribatti, Chick embryo chorioallantoic membrane as a useful tool to study angiogenesis, Int. Rev. Cell Mol. Biol. 270 (2008) 181–224.
[29] A. Vailaya, P. Bluvas, R. Kincaid, A. Kuchinsky, M. Creech, A. Adler, An architecture for biological information extraction and representation, Bioinformatics 21 (2005) 430–438.
[30] G.D. Bader, C.W. Hogue, An automated method for finding molecular complexes in large protein interaction networks, BMC Bioinformatics 4 (2003) 2.
[31] J. Chen, E.E. Bardes, B.J. Aronow, A.G. Jegga, ToppGene Suite for gene list enrichment analysis and candidate gene prioritization, Nucleic Acids Res. 37 (2009) W305–W311.
[32] S. Fan, Q. Geng, Z. Pan, X. Li, L. Tie, Y. Pan, X. Li, Clarifying off-target effects for torcetrapib using network pharmacology and reverse docking approach, BMC Syst. Biol. 6 (2012) 152.
[33] R.F. Machado, D. Laskowski, O. Deffenderfer, T. Burch, S. Zheng, P.J. Mazzone, T. Mekhail, C. Jennings, J.K. Stoller, J. Pyle, J. Duncan, R.A. Dweik, S.C. Erzurum, Detection of lung cancer by sensor array analyses of exhaled breath, Am. J. Respir. Crit. Care Med. 171 (2005) 1286–1291.
[34] B. Hamrita, K. Chahed, M. Trimeche, C.L. Guillier, P. Hammann, A. Chaieb, S. Korbi, L. Chouchane, Proteomics-based identification of alpha1-antitrypsin and haptoglobin precursors as novel serum markers in infiltrating ductal breast carcinomas, Clin. Chim. Acta 404 (2009) 111–118.
[35] Z. Sun, P. Yang, Role of imbalance between neutrophil elastase and alpha 1-antitrypsin in cancer development and progression, Lancet Oncol. 5 (2004) 182–190.
[36] A.M. Houghton, D.M. Rzymkiewicz, H. Ji, A.D. Gregory, E.E. Egea, H.E. Metz, D.B. Stolz, S.R. Land, L.A. Marconcini, C.R. Kliment, K.M. Jenkins, K.A. Beaulieu, M. Mouded, S.J. Frank, K.K. Wong, S.D. Shapiro, Neutrophil elastase-mediated degradation of IRS-1 accelerates lung tumor growth, Nat. Med. 16 (2010) 219–223.
[37] R.R. Drake, L.H. Cazares, E.E. Jones, T.W. Fuller, O.J. Semmes, C. Laronga, Challenges to developing proteomic-based breast cancer diagnostics, OMICS 15 (2011) 251–259.
[38] B.L. Adam, A. Vlahou, O.J. Semmes, G.J. Wright, Proteomic approaches to biomarker discovery in prostate and bladder cancers, Proteomics 1 (2001) 1264–1270.
[39] E.T. Fung, G.J. Wright, E.A. Dalmasso, Proteomic strategies for biomarker identification: progress and challenges, Curr. Opin. Mol. Ther. 2 (2000) 643–650.
[40] Z.J. El-Akawi, F.K. Al-Hindawi, N.A. Bashir, Alpha-1 antitrypsin (alpha1-AT) plasma levels in lung, prostate and breast cancer patients, Neuro. Endocrinol. Lett. 29 (2008) 482–484.
[41] V. Urquidi, S. Goodison, S. Ross, M. Chang, Y. Dai, C.J. Rosser, Diagnostic potential of urinary alpha1-antitrypsin and apolipoprotein E in the detection of bladder cancer, J. Urol. 188 (2012) 2377–2383.
[42] N. Maurice, D.H. Perlmutter, Novel treatment strategies for liver disease due to alpha1-antitrypsin deficiency, Clin. Transl. Sci. 5 (2012) 289–294.
[43] Z.J. El-Akawi, A.M. Abu-Awad, A.M. Sharara, Y. Khader, The importance of alpha-1 antitrypsin (alpha1-AT) and neopterin serum levels in the evaluation of non-small cell lung and prostate cancer patients, Neuro. Endocrinol. Lett. 31 (2010) 113–116.
[44] Y. Xu, J. Zhang, J. Han, X. Pan, Y. Cao, H. Guo, Y. Pan, Y. An, X. Li, Curcumin inhibits tumor proliferation induced by neutrophil elastase through the upregulation of alpha1-antitrypsin in lung cancer, Mol. Oncol. 6 (2012) 405–417.
[45] K. Deacon, D. Onion, R. Kumari, S.A. Watson, A.J. Knox, Elevated SP-1 transcription factor expression and activity drives basal and hypoxia-induced vascular endothelial growth factor (VEGF) expression in non-small cell lung cancer, J. Biol. Chem. 287 (2012) 39967–39981.
[46] M. Shibuya, Structure and function of VEGF/VEGF-receptor system involved in angiogenesis, Cell Struct. Funct. 26 (2001) 25–35.

[47] A. Rozman, M. Silar, M. Kosnik, Angiogenin and vascular endothelial growth factor expression in lungs of lung cancer patients, Radiol. Oncol. 46 (2012) 354–359.
[48] R.K. Jain, D.G. Duda, J.W. Clark, J.S. Loeffler, Lessons from phase III clinical trials on anti-VEGF therapy for cancer, Nat. Clin. Pract. Oncol. 3 (2006) 24–40.
[49] P. Carmeliet, R.K. Jain, Molecular mechanisms and clinical applications of angiogenesis, Nature 473 (2011) 298–307.
[50] R.K. Jain, D.G. Duda, C.G. Willett, D.V. Sahani, A.X. Zhu, J.S. Loeffler, T.T. Batchelor, A.G. Sorensen, Biomarkers of response and resistance to antiangiogenic therapy, Nat. Rev. Clin. Oncol. 6 (2009) 327–338.
[51] E. Messadi, Z. Aloui, E. Belaidi, M.P. Vincent, E. Couture-Lepetit, L. Waeckel, J. Decorps, N. Bouby, A. Gasmi, H. Karoui, M. Ovize, F. Alhenc-Gelas, C. Richer, Cardioprotective effect of VEGF and venom VEGF-like protein in acute myocardial ischemia in mice: effect on mitochondrial function, J. Cardiovasc. Pharmacol. 63 (2014) 274–281.
[52] I. Jutooru, G. Chadalapaka, P. Lei, S. Safe, Inhibition of NFkappaB and pancreatic cancer cell and tumor growth by curcumin is dependent on specificity protein down-regulation, J. Biol. Chem. 285 (2010) 25332–25344.
[53] G.S. Sidhu, H. Mani, J.P. Gaddipati, A.K. Singh, P. Seth, K.K. Banaudha, G.K. Patnaik, R. K. Maheshwari, Curcumin enhances wound healing in streptozotocin induced diabetic rats and genetically diabetic mice, Wound Repair Regen. 7 (1999) 362–374.
[54] M.S. Kiran, V.B. Kumar, R.I. Viji, G.T. Sherin, K.N. Rajasekharan, P.R. Sudhakaran, Opposing effects of curcuminoids on serum stimulated and unstimulated angiogenic response, J. Cell. Physiol. 215 (2008) 251–264.
[55] R.K. Maheshwari, A.K. Singh, J. Gaddipati, R.C. Srimal, Multiple biological activities of curcumin: a short review, Life Sci. 78 (2006) 2081–2087.
[56] D. Thaloor, K.J. Miller, J. Gephart, P.O. Mitchell, G.K. Pavlath, Systemic administration of the NF-kappaB inhibitor curcumin stimulates muscle regeneration after traumatic injury, Am. J. Physiol. 277 (1999) C320–C329.
[57] R. Li, X. Qiao, Q. Li, R. He, M. Ye, C. Xiang, X. Lin, D. Guo, Metabolic and pharmacokinetic studies of curcumin, demethoxycurcumin and bisdemethoxycurcumin in mice tumor after intragastric administration of nanoparticle formulations by liquid chromatography coupled with tandem mass spectrometry, J. Chromatogr. B Anal. Technol. Biomed. Life Sci. 879 (2011) 2751–2758.